Watershed hydrograph model based on surface flow diffusion

Yang Yang[1] and Theodore A. Endreny[1]

[1] Based on the diffusion equation and Darcy's law, Criss and Winston (2008b) developed the one-parameter analytical subsurface flow diffusion hydrograph model to represent the theory of rapid displacement of "old" aquifer water and shallow pore water following rainfall events. We developed a two-parameter analytical surface flow diffusion hydrograph model for urban or other basins that generate surface runoff similar to flash floods following a sharp pulse of rainfall at the watershed inlet. The model uses two time parameters that are based on watershed scale, flow diffusivity, and flow celerity to control the shape of the hydrograph and time to discharge peak. The two-parameter analytical surface flow diffusion model was mathematically and experimentally compared with the one-parameter analytical subsurface diffusion hydrograph model proposed by Criss and Winston (2008b). We demonstrated that the one-parameter model represented one extreme case of the two-parameter model when the advection of subsurface flow was zero and that the two-parameter model was applicable for both surface and subsurface flow hydrograph simulations. The two-parameter model was tested on several watersheds and was shown to have a high efficiency in simulating hydrograph timing and peak discharge as well as in matching rising and falling limb inflection points. Fitting the two-parameter surface flow diffusion hydrograph model to a watershed runoff event helps to quantify the role of advective and diffusive transport on discharge and how it changes with changing storm and land cover characteristics.

1. Introduction

[2] The hydrograph for a rainfall event is generally composed of a mixture of subsurface flow and surface flow. By understanding the watershed controls on runoff, hydrologists can better separate subsurface and surface flows in hydrographs and predict runoff travel times, pollutant loads, and flood risk [*Rinaldo et al.*, 2011; *Smith and Ward*, 1998]. The need for hydrograph prediction is particularly critical for urban flash floods given their destruction of human life and property [*Younis et al.*, 2008] and their increasing frequency with increasing urbanization [*Hapuarachchi et al.*, 2011]. The intense convective rainfall-triggering flash floods [*Baeck and Smith*, 1998] is now forecasted with increasing accuracy extending out to 6 h [*Hapuarachchi et al.*, 2011]; however, model flood predictions remain inadequate [*Ntelekos et al.*, 2006]. The variety of methods developed for flood prediction demonstrates the associated importance and challenge of this task. Flood prediction methods include distributed rainfall runoff models with extensive or parsimonious parameters [*Beven and Binley*, 1992; *Brocca et al.*, 2011], artificial neural network models [*Hsu et al.*, 1995], unit or geomorphological instantaneous unit hydrograph models [*Javier et al.*, 2007], threshold runoff estimation mapping models [*Carpenter et al.*, 1999], and stochastic and Bayesian methods for the above models [*Georgakakos*, 1986; *Krzysztofowicz*, 1999; *Martina et al.*, 2005; *Ntelekos et al.*, 2006]. Flood model accuracy is most sensitive to errors in rainfall intensity and distribution [*Javier et al.*, 2007; *Ogden et al.*, 2000]; however, each modeling approach is also constrained by parameter estimation of basin infrastructure, which is constrained by observational networks [*Javier et al.*, 2007; *Ogden et al.*, 2011; *Younis et al.*, 2008]. Parsimonious models provide an appealing approach to improve hydrograph prediction if they can integrate basin infrastructure and geomorphic complexity into a few representative parameters and handle short forecast lead times.

[3] Development of a parsimonious hydrograph model capable of generating accurate flood forecasts is motivated by the recent success of a subsurface flow diffusion method in predicting another complex runoff phenomenon. For subsurface flow, hydrologists have theorized rainfall triggers a pressure wave displacement of preexisting "old" saturated and unsaturated pore water [*McDonnell*, 1990]. *Criss and Winston* [2003, 2008a, 2008b] attempted to simulate the rapid displacement of old water by developing a one-parameter subsurface flow diffusion hydrograph model of the rainfall triggered pressure wave. Their one-parameter

[1]Environmental Resources Engineering, College of Environmental Science and Forestry, State University of New York, Syracuse, New York, USA.

Corresponding author: T. A. Endreny, Environmental Resources Engineering, College of Environmental Science and Forestry, State University of New York, 404 Baker Labs, 1 Forestry Drive, Syracuse, NY 13210-2773, USA. (te@esf.edu)

subsurface flow diffusion model had a single time parameter, which reflects the basin-scale and soil characteristics and fits the predicted hydrograph to the natural hydrograph properties of time to peak, total flow volume, inflection points, and recession rate [*Criss and Winston*, 2008b]. *Criss and Winston* [2008b] applied the one-parameter subsurface flow diffusion model on several small humid watersheds and demonstrated that their model was simpler and performed better than common alternatives, such as the unit hydrograph and linear reservoir exponential model. However, the theoretical basis of the model is the subsurface flow diffusion equation and Darcy's law, which limits the application of the model to hydrographs generated by subsurface flow. Model test results showed that the one-parameter subsurface flow diffusion model worked better on rural watersheds than on urbanized watersheds where surface flow may be significant [*Criss and Winston*, 2008a].

[4] Surface flow by saturation or infiltration excess can significantly regulate the hydrograph in basins of particular morphologies and surficial materials, such as urban and other impervious watersheds, or under particular rainfall conditions, such as high-intensity rains or antecedent moisture conditions [*Easton et al.*, 2007; *Winchell et al.*, 1998]. Simulation of these surface runoff phenomena can follow the same theoretical approach used by the one-parameter subsurface flow diffusion model. In this research, we established an analytical two-parameter surface flow diffusion hydrograph model based on the analytical solution to the surface flow advection-diffusion equation [*Yen and Tsai*, 2001]. The analytical two-parameter surface flow diffusion hydrograph model was developed for a pulse input of effective rainfall at the upstream watershed boundary, similar to the boundary condition used by *Criss and Winston* [2003, 2008a, 2008b] in their subsurface flow diffusion hydrograph model. We provided a parameter sensitivity analysis of the model, compared the two-parameter surface flow diffusion hydrograph model with the one-parameter subsurface flow diffusion model, and proposed the possible extension of the one-parameter model to the two-parameter model. We then demonstrated applications of the two-parameter diffusion model to simulate hydrographs for urban watersheds after intense rainfall.

2. Two-Parameter Analytical Surface Flow Diffusion Hydrograph Model

2.1. Model Development

[5] In hydrology and hydraulics, the dynamic equations, also known as the St. Venant equations [*Saint-Venant*, 1871], are widely used to simulate channel flow or surface flow with different levels of wave approximations: the kinematic wave, noninertia wave, gravity wave, and quasi-steady dynamic wave. The advection-diffusion equation is also used to simulate the transport of a wave disturbance along the runoff pathway such as a river or over land surface. *Yen and Tsai* [2001] demonstrated physically and mathematically that the advection-diffusion equation can be formulated from different levels of wave approximations of the dynamic equations under the assumption that the wave celerity and hydraulic diffusivity are stepwise constant. Here, we use the generalized advection-diffusion equation defined by *Yen and*
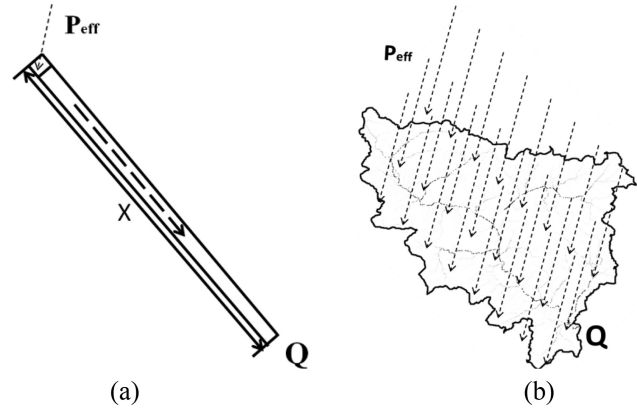
Figure 1. Sketch of a (a) linear ideal watershed modeled by equation and (b) nonideal or real irregularly shaped watershed.

Tsai [2001] to describe the one-dimensional channel flow and surface flow in a linear ideal watershed (Figure 1a):

$$\frac{\partial Q}{\partial t} + c\frac{\partial Q}{\partial x} = D\frac{\partial^2 Q}{\partial x^2}. \tag{1}$$

[6] In equation (1), Q (L^3/t) is the flow rate at a distance x (L) downstream from the point $x = 0$, where the effective precipitation P_{eff} (L) happens, c (L/t) is the kinematic wave celerity, and D (L^2/t) is the diffusivity that reflects the tendency of the water wave to disperse longitudinally as it travels downstream. P_{eff} is the available water for surface runoff after the deduction of evapotranspiration, infiltration, canopy interception, depression storage, and any other water loss from the total precipitation. Assuming c and D are constants and P_{eff} is a pulse disturbance, an analytical solution for equation (1) can be obtained as follows:

$$Q(x,t) = \frac{P_{\text{eff}} \times A}{2\sqrt{\pi D}} x t^{-\frac{3}{2}} e^{-\frac{(x-ct)^2}{4Dt}}, \tag{2}$$

where *Brutsaert* [2005] presented equation (2) for discharge velocity, not discharge volume, and used a unit value for P_{eff}. A (L^2) is the watershed surface area receiving the P_{eff}. The exponential term of equation (2) approximates the Gaussian distribution with ct as the mean and $2Dt$ as the variance (the whole equation is an inverse Gaussian distribution). This indicates that the main body of the surface flow moves to the outlet with a celerity c and with a dispersion of D.

[7] The timing of the runoff peak, $t_{\max}$, is determined by differentiating Q in equation (2) with respect to t, which gives $t_{\max} = \frac{1}{2c^2}\left(-6D + 6D\sqrt{1 + \frac{x^2 c^2}{9D^2}}\right)$. With $t_{\max}$, we can determine $Q_{\max}$. Equations for $t_{\max}$ and $Q_{\max}$ are written as the function of two time constant parameters, α and β:

$$t_{\max} = -\frac{3}{4}\alpha + \frac{3}{4}\alpha\sqrt{1 + \frac{16}{9}\frac{\beta}{\alpha}}, \tag{3}$$

$$Q_{\max} = \frac{P_{\text{eff}} \times A}{\sqrt{\pi}}\sqrt{\beta} \times t_{\max}^{-\frac{3}{2}} e^{-\frac{\beta}{t_{\max}}} e^{-\frac{t_{\max}}{\alpha}} e^{2\sqrt{\frac{\beta}{\alpha}}}, \tag{4}$$

$$\alpha = \frac{4D}{c^2}, \tag{5}$$

$$\beta = \frac{x^2}{4D}. \tag{6}$$

[8] The normalized discharge at any time is obtained by taking the quotient of equations (2) and (4), and this formulation facilitates intercomparison of hydrographs.

$$\frac{Q}{Q_{max}} = \left(\frac{t}{t_{max}}\right)^{-\frac{3}{2}} e^{-\beta\left(\frac{1}{t} - \frac{1}{t_{max}}\right)} e^{-\frac{1}{\alpha}(t - t_{max})}. \tag{7}$$

[9] To obtain the surface diffusion wave hydrograph for an irregularly shaped, nonideal watershed (Figure 1b), we allow P_{eff} to occur everywhere in the watershed and integrate the normalized surface flow diffusion hydrographs of all the individual areal elements. By assuming that the values of P_{eff} and α are homogeneous for the whole watershed, the normalized hydrograph at the outlet can be simulated by the following equation:

$$\frac{Q^*}{Q^*_{max}} = F \times \frac{\int_0^A \frac{Q}{Q_{max}} dA}{\int_0^A dA}, \tag{8}$$

where F is a scaling parameter to set the right-hand side maximum to 1 (the introduction of F is due to the likelihood the maximum flow from different element areas reaches the watershed outlet at different times), Q^* is the discharge rate at the outlet, Q^*_{max} is the maximum discharge rate at the outlet, and Q and Q_{max} represent the discharge rate and maximum discharge rate generated by a particular areal element of area dA.

[10] The term areal element, dA, in equation (8) relates to the flow path length x, as $dA = l \times x^n dx$, in which l is a constant relating x and dA and n represents the projected geometry of the watershed area, such as $n = 1$ for a linear watershed and $n = 2$ for a pie-shaped watershed [*Criss and Winston*, 2008b]. Parameter n is a real number and can be obtained from the analysis of the flow length versus flow area graph. Given that equation (6) equates β to x and D, and setting D to a constant in the watershed, dA can be written in terms of β instead of x: $dA = 2^{n+1} l \times D^{(n+1)/2} \beta^{(n-1)/2} d\beta$, then equation (8) can be transformed by integration of β:

$$\frac{Q^*}{Q^*_{max}} = F \times \frac{\int_0^{\beta_{max}} \frac{Q}{Q_{max}} \beta^{\frac{n-1}{2}} d\beta}{\int_0^{\beta_{max}} \beta^{\frac{n-1}{2}} d\beta}, \tag{9}$$

where β_{max} represents the maximum β value among the areal elements.

[11] The integrated surface flow diffusion hydrograph of equation (9) gives more control over the timing of the rising and falling limb than the nonintegrated surface flow diffusion hydrograph of equation (7). The integrated hydrograph explicitly considers each watershed areal element and therefore simulates a more rapid runoff response from areas near
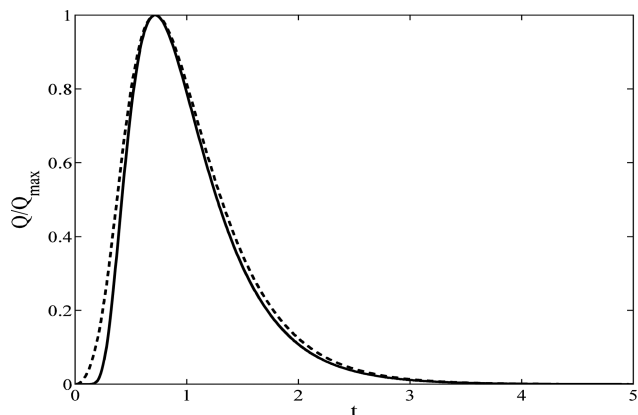
Figure 2. Integrated (dashed line) and nonintegrated (solid line) normalized surface flow diffusion hydrographs for $\alpha = 0.5$, $\beta = 7.1$, and $\beta_{max} = 10$. The $\beta = 7.1$ term was set to keep t_{max} the same for the two hydrographs.

the outlet and a more delayed runoff response from distant areas. Therefore, the integrated hydrograph allows for an earlier rising limb as well as a later falling limb when compared with the nonintegrated hydrograph (Figure 2). Similar differences were observed between the integrated and the nonintegrated forms of the subsurface flow diffusion hydrograph [*Criss and Winston*, 2008a]. The integrated form (equation (9)) requires complicated numerical calculation, whereas the nonintegrated form (equation (7)) is a simpler calculation, and by adjusting the β value, it provides the same t_{max} and similarly shaped rising and falling limbs as the integrated form (Figure 2). Thus, if the modeler can accept a slightly delayed rising limb and slightly premature falling limb in the hydrograph, the simpler nonintegrated surface flow diffusion hydrograph (equation (7)) with lumped α and β values is recommended to simulate the whole watershed. In this paper, we apply the nonintegrated hydrograph model for all the simulations.

[12] The surface flow diffusion hydrograph model of equation (2) and its normalized version of equation (7) provide an analytical framework that facilitates examination of watershed runoff response to rainfall impulses. From this framework, we can compute the total amount of water transported in response to a given rainfall pulse by integrating Q in equation (2) over all time, which is equal to the product $\sqrt{\pi/\beta} \times t_{max}^{3/2} Q_{max} \exp\left(\beta/t_{max} + t_{max}/\alpha - 2\sqrt{\beta/\alpha}\right)$ (see the Appendix A for the integral process). The analysis of equations (2) and (7) reveals that the hydrograph falling limbs at very long times take the form of $t^{-2/3}$.

2.2. Sensitivity Analysis

[13] Development of the analytical form of the two-parameter surface flow diffusion hydrograph model provides a predictable sensitivity of the time to peak t_{max}, peak discharge Q_{max}, and rising limb proportion (RLP) (or falling limb proportion) to the time parameters α and β. The RLP is calculated as the integral of equation (7) with respect to t from 0 to t_{max}. The sensitivity of t_{max}, Q_{max}, and RLP to α and β is obtained by taking the partial derivative of α and β (Figure 3).
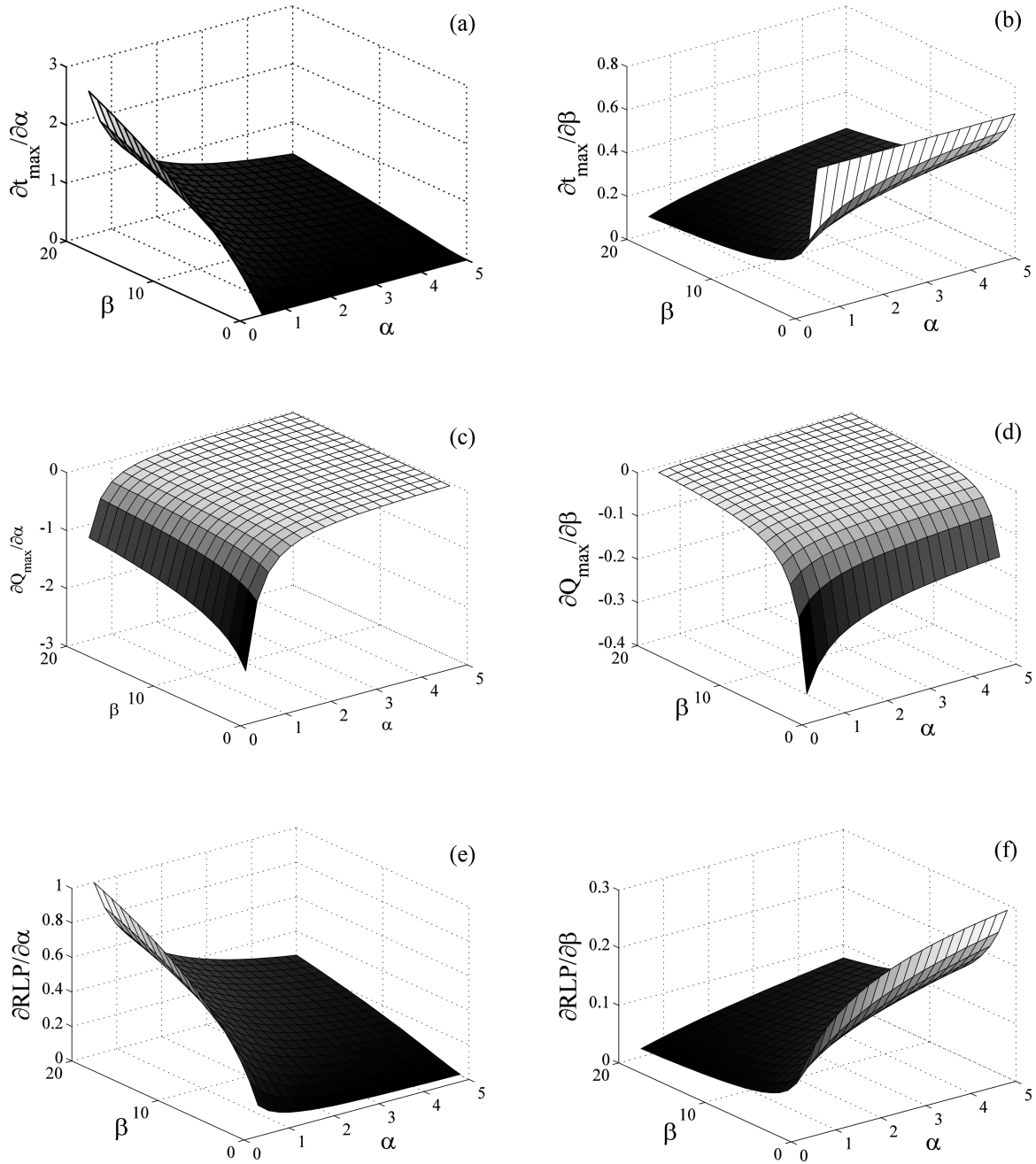
Figure 3. Sensitivity analysis of (a) t_{max} to α, (b) t_{max} to β, (c) Q_{max} to α, (d) Q_{max} to β, (e) RLP to α, and (f) RLP to β.

[14] For t_{max}, (a) when β is fixed, t_{max} increases with the increase of α ($\partial t_{max}/\partial\alpha > 0$), whereas the rate of increase (the absolute value of $\partial t_{max}/\partial\alpha$) decreases with the increase of α (becomes less sensitive to α as α increases; Figure 3a); (b) when α is fixed, t_{max} increases with the increase of β ($\partial t_{max}/\partial\beta > 0$), whereas the rate of increase (the absolute value of $\partial t_{max}/\partial\beta$) also decreases with the increase of β (Figure 3b). The amplitude of $\partial t_{max}/\partial\alpha$ is larger than the amplitude of $\partial t_{max}/\partial\beta$, which indicates that t_{max} is more sensitive to α than to β.

[15] For Q_{max}, (c) when β is fixed, Q_{max} decreases with the increase of α ($\partial Q_{max}/\partial\alpha < 0$), whereas the rate of decrease (the absolute value of $\partial Q_{max}/\partial\alpha$) decreases with

the increase of α (Figure 3c); (d) when α is fixed, Q_{max} decreases with the increase of β ($\partial Q_{max}/\partial\beta < 0$), whereas the rate of decrease (the absolute value of $\partial Q_{max}/\partial\beta$) decreases with the increase of β (Figure 3d). The amplitude of $\partial Q_{max}/\partial\alpha$ is larger than the amplitude of $\partial Q_{max}/\partial\beta$, which indicates that Q_{max} is more sensitive to α than to β.

[16] For RLP, (e) when β is fixed, RLP increases with the increase of α ($\partial RLP/\partial\alpha > 0$), whereas the rate of increase (the absolute value of $\partial RLP/\partial\alpha$) decreases with the increase of α (Figure 3e); (f) when α is fixed, RLP increases with the increase of β ($\partial RLP/\partial\beta > 0$), whereas the rate of increase (the absolute value of $\partial RLP/\partial\beta$) decreases with the increase of β (Figure 3f). The amplitude of $\partial RLP/\partial\alpha$ is larger than

the amplitude of ∂RLP/∂β, which indicates that RLP is more sensitive to α than to β.

[17] A visual demonstration of the influence of α and β on the normalized hydrograph is shown in Figure 4. Setting $\beta = 1$ and varying α from 0.1 to infinity, α and β together determine the rising limb, $t_{\max}$, and falling limb when α is small (Figure 4a); as α decreases, the faster the rising and falling limb and the smaller $t_{\max}$. When α is large (>10), β determines the hydrograph shape and $t_{\max} \approx 2\beta/3$. Setting $\alpha = 1$ and varying β from 0.1 to 100, the normalized hydrographs series indicate that β always contributes to $t_{\max}$ and the hydrograph elongates as β becomes large (Figure 4b).

3. Comparison with One-Parameter Subsurface Flow Diffusion Hydrograph Model

3.1. Mathematical Comparison

[18] Based on aquifer water head diffusion equation and Darcy's law, *Criss and Winston* [2008b] developed the one-parameter analytical subsurface flow diffusion hydrograph model to represent the theory of rapid displacement of old aquifer water and shallow pore water following rainfall events. The normalized subsurface flow diffusion hydrograph

Figure 4. Normalized surface flow diffusion hydrographs modeled for (a) five α values from 0.1 to $+\infty$ with a fixed $\beta = 1$ and (b) four β values from 0.1 to 100 with a fixed $\alpha = 1$.

model [*Criss and Winston*, 2003] can be described by the following equation:

$$\frac{Q}{Q_{\max}} = \left(\frac{t}{t_{\max}}\right)^{-\frac{3}{2}} e^{-b\left(\frac{1}{t} - \frac{1}{t_{\max}}\right)}. \qquad (10)$$

where $b = x^2/(4D)$, in which x is the watershed scale, D is the diffusivity of subsurface flow, and $t_{\max} = 2b/3$. Note that b is equivalent to β in the two-parameter surface flow diffusion model.

[19] A visual comparison of equations (7) and (10) reveals similarities between the two-parameter diffusion model and the one-parameter diffusion model. The only difference is the additional exponential term $e^{-\frac{1}{\alpha}(t - t_{\max})}$ in equation (7), which represents the kinematic flow of the water. This exponential term also exists in the exponential and gamma function models [*Criss and Winston*, 2008b]. When α approaches infinity (the kinematic flow celerity is 0), the exponential term goes to 1, and the two-parameter surface flow diffusion hydrograph model has the same form of the one-parameter subsurface flow diffusion hydrograph model. Therefore, the form of the subsurface flow diffusion hydrograph model represents one extreme condition of the surface flow diffusion hydrograph model. Many studies have demonstrated that subsurface flow has advection behavior [*Deming et al.*, 1992; *García et al.*, 2004; *Kirchner et al.*, 2001], suggesting that it is reasonable to add the advection term to subsurface flow and that the one-parameter diffusion hydrograph model can be extended to the two-parameter diffusion hydrograph model.

[20] When compared with the one-parameter diffusion model, the two-parameter diffusion model has more flexibility in representing hydrograph shapes; when $t_{\max}$ is fixed, there are an infinite set of α and β value pairs that give the same $t_{\max}$ (Figure 5). Each set of α and β value pairs will determine the hydrograph shape (Figure 6). Although the simulated hydrographs have different shapes, they all have the characteristics of natural hydrographs, such as a relatively fast rising limb, a relatively gradual falling limb, and one inflection point in the rising limb and falling limb. The rising limb flow fraction of total runoff is fixed for the one-parameter diffusion hydrograph model at 0.0833, whereas it can range from 0.0833 to 0.5 for the two-parameter
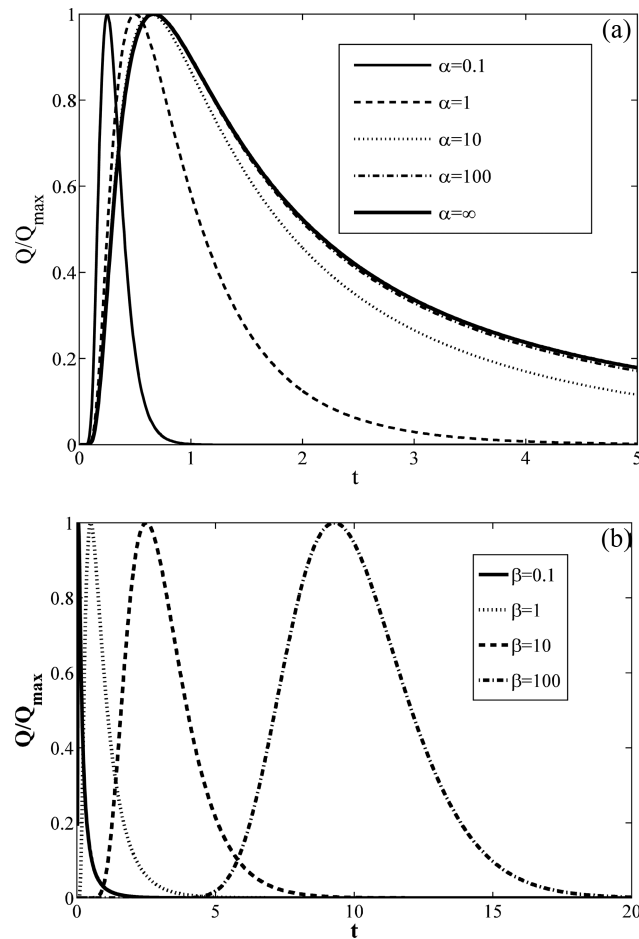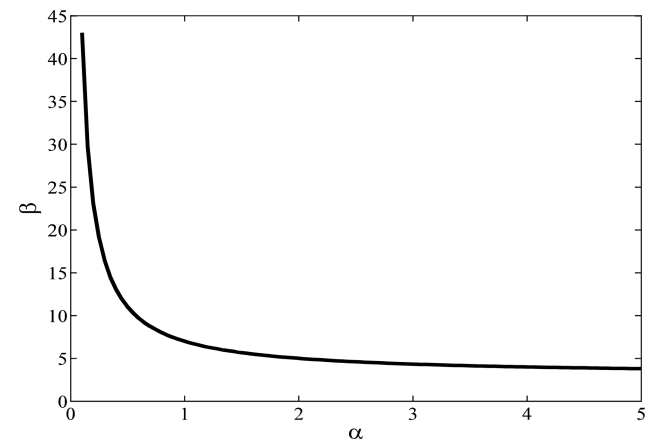
Figure 5. The α and β value pairs where $t_{\max} = 2$ h representing the rate of change in α and β for value pair.
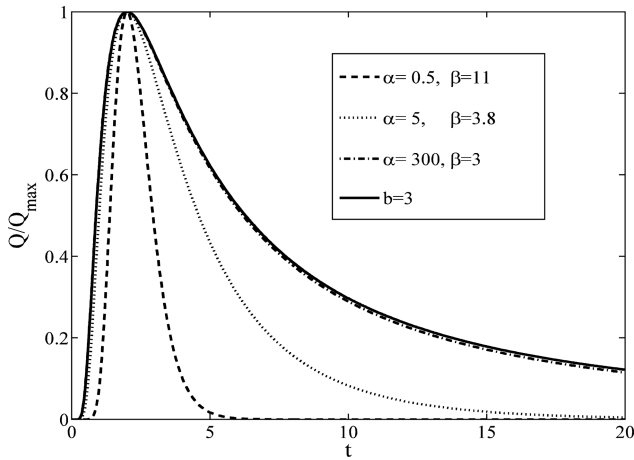
Figure 6. Normalized surface flow diffusion hydrographs modeled for different values of α and β with $t_{max} = 2$ h. When $\alpha = 300$ and $\beta = 3$, the surface flow diffusion hydrograph overlaps the subsurface flow diffusion hydrograph, denoted with $b = 3$.

diffusion hydrograph model, which can better represent the reported range from 0.07 to 0.35 for natural hydrographs [*Criss and Winston*, 2008b].

3.2. Experimental Comparison

[21] *Criss and Winston* [2008b] applied the one-parameter diffusion hydrograph model to fit the long-term observed hydrograph for two nearby watersheds Williams Creek near

Peerless Park, MO (USGS 07019090) and Fishpot Creek at Valley Park, MO (USGS 07019120) (Figure 7). The two watersheds have very different basin characteristics: Fishpot Creek at Valley Park is a highly urbanized 24.8 km^2 watershed, whereas Williams Creek near Peerless Park is a forested 19.7 km^2 watershed. The calibrated time constant for Williams Creek near Peerless Park was 1 day, whereas the time constant for Fishpot Creek at Valley Park was just 0.05 days. For Williams Creek near Peerless Park, the one-parameter diffusion hydrograph model had a much better fit with the observed hydrograph, as recorded with a higher Nash-Sutcliff efficiency (NSE) [*Nash and Sutcliffe*, 1970] of 0.605 than 0.135 for Fishpot Creek at Valley Park. *Criss and Winston* [2008b] attributed the lower NSE to the flashy response of Fishpot Creek at Valley Park due to its sensitivity to rainfall heterogeneity. We suggested that the low NSE at Fishpot Creek at Valley Park can be attributed to the limitations of the one-parameter hydrograph model in capturing the fast falling limb typical for urbanized watersheds. To illustrate this point, we applied both one-parameter hydrograph model and two-parameter hydrograph model to Fishpot Creek at Valley Park for the intense 12 mm/h rain storm in 9 April 2001. The rain data were from the National Oceanic and Atmospheric Administration (NOAA) station at CAHOKIA/St. Louis (WBAN: 725314 99999) with a temporal resolution of 1 h, and the discharge data were from USGS gauging station 07019120 with temporal resolution of 5 min. The simulations were done at 5 min time interval by assuming that the rainfall happened in the exact hour. When the one- and two-parameter models have the same
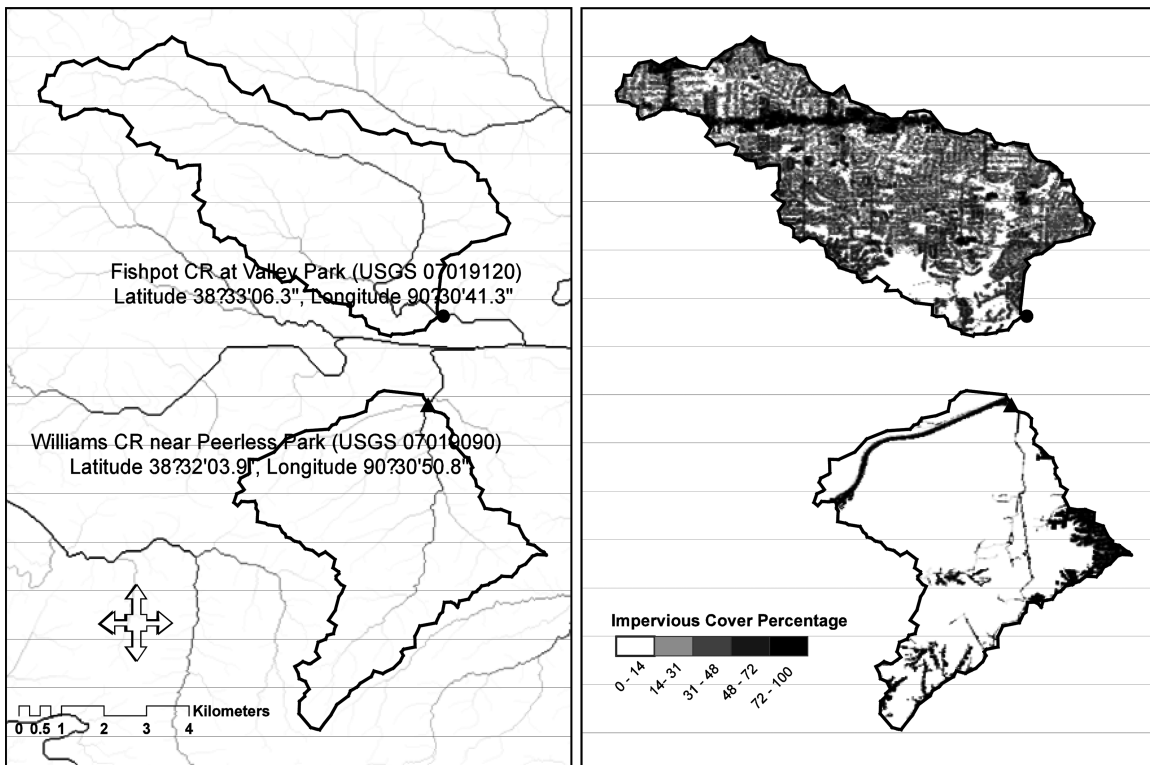
Figure 7. (top) Watersheds of Fishpot Creek at Valley Park, MO and (bottom) Williams Creek near Peerless Park, MO. (left) Watershed boundaries and drainage. (right) The NLCD 2001 estimates of impervious land cover percentages in the two watersheds.
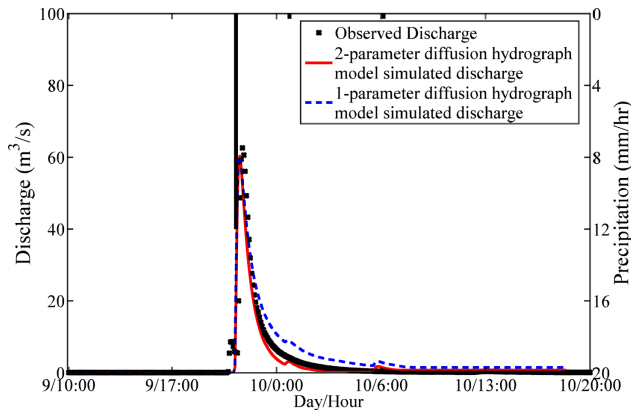
Figure 8. One-parameter diffusion hydrograph model and two-parameter diffusion hydrograph model predictions and the observed hydrograph for the rain events between 9 and 10 April 2001 at Fishpot Creek at Valley Park, MO.

simulated t_{max} and rising limb, the two-parameter diffusion hydrograph model was able to better simulate the rapid hydrograph recession (Figure 8). This is attributed to model formulation rather than the extra degree of freedom for the two-parameter model versus the one-parameter model.

4. Applications

[22] The two-parameter diffusion hydrograph model was further applied on four urban watersheds: Green Brook at Seeley Mills, NJ (USGS 01403400, area 16.1 km^2); Rock Creek at Sherrill Drive Washington, DC (USGS 01648000,

area 161.1 km^2); Crabtree Creek at US 1 at Raleigh, NC (USGS 02087324, area 313.4 km^2); and Salado Creek at Loop 13, TX (USGS 08178800, area 489.5 km^2). The four watersheds are classified as urban by the National Water Quality Assessment program data warehouse according to the dominant land cover influencing the watershed. We hypothesized that surface runoff dominates the discharge after intense rainfall for these watersheds. The discharge data are from USGS gauging stations with temporal resolution of 15 min, and the rain data are from their nearby NOAA weather stations with temporal resolution of 1 h (Figure 9). The simulations were done at 15 min time interval by assuming that the rainfall happened in the exact hour. The two time constants α and β and a scale parameter that scaled the normalized hydrograph to the observed discharge peak were calibrated by the Model-Independent Parameter Estimation & Uncertainty Analysis software (PEST) [*Doherty*, 2001] using the Gauss-Marquardt-Levenberg algorithm, which integrates the advantages of the inverse Hessian method and the steepest descent method [*Press et al.*, 1986]. The optimized objective function is the weighted sum of squared differences between model-simulated discharge and the observed discharge. The timing of the peaks and the falling limbs were simulated very well, and the simulated hydrographs had very high NSE values, although the simulated rising limbs and peak amplitudes did not fit the observed hydrographs perfectly (Figure 9). The rising limb simulation is sensitive to the time of rainfall, and the hourly time step for rain data is too coarse to capture 15 min time step in the runoff response. Finer resolution rainfall data from within the watershed would likely improve the runoff simulation; however, these data were
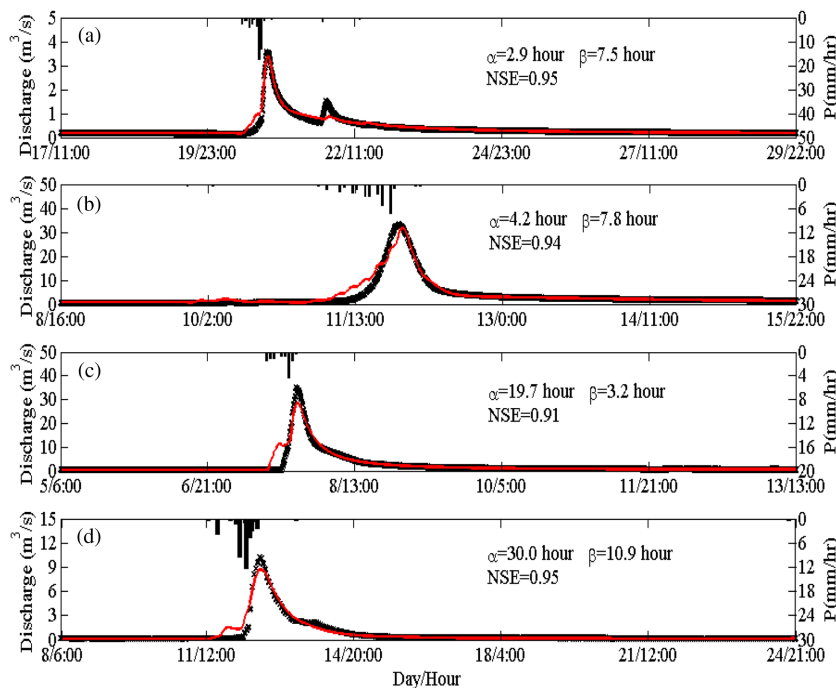
Figure 9. Surface flow diffusion hydrograph model predictions (solid red line) and the observed hydrograph (star marker) for four urban watersheds: (a) Green Brook at Seeley Mills, NJ, 17–29 April 2009; (b) Rock Creek at Sherrill Drive Washington, DC, 8–15 December 2008; (c) Crabtree Creek at US 1 at Raleigh, NC, 5–13 September 2009; and (d) Salado Creek at Loop 13, TX, 8–24 March 2009.

not available. The peak discharge simulation underestimated observed peaks due to our use of a single-scale parameter to compute P_{eff} for each watershed for all rain events. We could reduce this error by changing the percentage of rainfall that becomes P_{eff} during the events; however, this detracts from our presentation of equation (7) and introduces the separate issue of initial abstractions.

5. Discussion

[23] This research developed an analytical two-parameter surface diffusion hydrograph model for urban and similar basins with significant overland flow to improve storm hydrograph prediction, represent the runoff mechanisms with the model parameters, and maintain a parsimonious approach to process simulation. The two time-based parameters used by the model represent watershed scale, flow diffusivity, and flow celerity. Alternative two-parameter models based on probability functions are equally parsimonious; however, the parameters do not represent runoff mechanisms. For example, *Hrachowitz et al*. [2010] found that the two parameters of the gamma function were sensitive to a wide range of catchment characteristics and climate; however, the parameters of the gamma function or any other probability function have no physical relationship with catchment characteristics. In contrast, the two time constants α and β of the surface diffusion model have direct physical representation of watershed and weather controls on runoff and hydrograph features. A Geographic Information Systems (GIS)-based analysis has documented how surface runoff celerity and diffusivity change with varying rain intensity, land cover, and land slope [*Liu et al*., 2003], which demonstrates how α and β values are physically representative of watershed and rainfall characteristics. This research determined the parameters α and β using inverse-model calibration and illustrated parameter sensitivity to rainfall and watershed characteristics. Subsequent research should explore methods to derive these physically based parameters from watershed and storm based indices, analytical relationships, or regression models [*Chaplot and Walter*, 2003; *Lee et al*., 2007; *Vogel and Kroll*, 1992].

[24] Urbanized watersheds have short time of concentration, making them vulnerable to flash flooding during intense rains [*Baeck and Smith*, 1998], and as urbanization expands, more people are threatened by such flash floods [*Hapuarachchi et al*., 2011]. Parsimonious models are considered to be better suited to handle flash flood and real-time forecasting given the complexity and uncertainty in urban runoff dynamics [*Young*, 2002], particularly with ongoing changes to impervious cover and stormwater infrastructure [*Marsalek and Chocat*, 2002]. Overparameterized models are less efficient and have greater validation challenges and uncertainty than parsimonious models, particularly in responding to variations in time-series rainfall [*Perrin et al*., 2001]. For flash flood events with short rainfall durations, our two-parameter diffusion hydrograph model was highly sensitive to the quality and time resolution of the rainfall data. This model sensitivity to rainfall accuracy during urban flash floods was also present in the spatially distributed models [*Ogden et al*., 2000], simple infiltration models, and geomorphological instantaneous unit hydrograph models [*Javier et al*., 2007]. *Javier et al*. [2007]

explained how individual bridges and other in-stream infrastructure had significant control on hydrograph peak discharge and timing, an influence our surface diffusion hydrograph model might represent by with its celerity parameter.

[25] Hydrograph simulation can inform watershed management when used for historical analysis of runoff processes and controls as well as in a predictive flood forecasting mode. This value of historic prediction was demonstrated by *Ogden et al*. [2011] when they analyzed how a range of possible surface and subsurface drainage scenarios affected flood severity for a historic flash flood in Baltimore, MD. In our application of the two-parameter model, we focused on historical analysis and to scale the simulated normalized hydrograph to match the observed discharge and then considered watershed controls α and β values and resulting time to peak and hydrograph inflection points. To apply the model in forecast mode for a particular watershed, historical simulations should be completed to identify suitable α and β values for different classes of effective precipitation. This process can follow a typical calibration and validation process [*Refsgaard*, 1997]. For subsequent forecasts of effective precipitation, the parameter values associated with the specific rainfall classes would be used to estimate the flood hydrograph. Then the peak discharge Q_{max} can be calculated based on equation (4), and Q at any time can be predicted based on equation (7).

[26] The two-parameter diffusion hydrograph model was developed and applied to urbanized watersheds where it was assumed surface flow dominates the hydrograph response. However, as we illustrated above, the one-parameter subsurface diffusion flow model can be extended to the two-parameter diffusion model, which makes the two-parameter model applicable for simulating events dominated by subsurface flow. By assigning the surface flow and the subsurface flow with the same time constants α and β, the two-parameter model can be applied to simulate discharge with mixed surface flow and subsurface flow. When surface flow and subsurface flow have different time constants α and β, a parallel model that consists of two two-parameter models can be constructed to simulate the hydrograph. As urban watersheds are retrofitted and redesigned with permeable pavement [*Sansalone et al*., 2008] and green infrastructure [*Marsalek and Chocat*, 2002; *Schilling and Logan*, 2008], stormwater will recharge the groundwater [*Endreny and Collins*, 2009] and change the percentage of surface and subsurface flow in urban hydrographs [*Black and Endreny*, 2006]. To facilitate hydrograph prediction and analysis in urban watersheds, the two-parameter surface diffusion hydrograph model is being incorporated into the iTree Hydro model, a tool designed to help cities manage stormwater [*Yang et al*., 2011]. The application of our surface diffusion hydrograph model in a parallel mode to simulate surface and subsurface will allow cities to assess how green infrastructure and stormwater interventions influence the timing, peak, and recession characteristics of urban flood hydrographs.

6. Conclusions

[27] We developed a two-parameter surface flow diffusion hydrograph model based on the analytical solution for the advection-diffusion equation describing the surface flow. This model uses only two parameters, the watershed time constants α and β, to simulate the shape of the

hydrograph, rising and falling limbs, and the timing of the peak. The time constants α and β carry the information of the watershed scale, surface flow diffusivity, and flow celerity. The previously developed one-parameter subsurface flow diffusion model is a specific case of the surface flow diffusion model, in which the exponential term reflecting the effect of flow celerity is equal to 1 (flow celerity is 0). Both hydrograph models provide excellent representation of natural hydrograph characteristics, including the inflection points in the rising and falling limbs, a fast rising limb and a gradual falling limb, and time to peak. The normalized two-parameter surface flow diffusion hydrograph model can be used directly for hydrograph prediction with a scaling parameter to match the observed discharge. The applications of the normalized two-parameter surface flow diffusion model on urban watersheds showed that it can simulate hydrograph timing and peak discharge as well as rising and falling limb inflection points.

Appendix A: Integral of the Hydrograph Function

[28] To obtain the total amount of water transported in response to a given rainfall pulse, we integrate Q in equation (2) over time. Based on the normalized hydrograph equation (7), Q can be represented by $Q = Q_{\max}(t_{\max})^{\frac{3}{2}}$ $e^{\frac{\beta}{t_{\max}}}e^{\frac{t_{\max}}{\alpha}}t^{-\frac{3}{2}}e^{-\frac{\beta}{t}}e^{-\frac{t}{\alpha}}$, in which terms $t^{-\frac{3}{2}}e^{-\frac{\beta}{t}}e^{-\frac{t}{\alpha}}$ are relevant to t and the integral of Q with time t is reduced to the integral $\int_0^\infty t^{-\frac{3}{2}}e^{-\frac{\beta}{t}}e^{-\frac{t}{\alpha}}dt$. We used the saddle point method to evaluate this integral, which is recognized as the Laplace transform of $t^{-\frac{3}{2}}e^{-\frac{\beta}{t}}$. The principle of the saddle point method is illustrated as follows. For an integral like $I(s) = \int_a^b g(z)e^{sf(z)}dz$, the exponential function makes a sharp peak for the integrand at z_0, which is the extreme point of the function $f(z)$. The only significant contribution to the integral comes from the immediate vicinity of the extreme point $z = z_0$ [*Arfken et al.*, 2012]. Therefore, the integral result is approximated by the expression $I(s) = \frac{\sqrt{2\pi}g(z_0)e^{sf(z_0)}}{|sf''(z_0)|^{1/2}}$, where only the information about the position of the extreme point of $f(z)$ and the second-order derivative $f(z)$ at z_0 is required. In the integral in our case, we have $g(t) = t^{-\frac{3}{2}}$, $f(t) = -\frac{\beta}{t} - \frac{t}{\alpha}$, and the extreme point $t_0 = \sqrt{\alpha\beta}$. Calculation shows that $\int_0^\infty t^{-\frac{3}{2}}e^{-\frac{\beta}{t}}e^{-\frac{t}{\alpha}}dt = \sqrt{\frac{\pi}{\beta}}e^{-2\sqrt{\frac{\beta}{\alpha}}}$ and the integral of Q with time t from 0 to ∞ equals $\sqrt{\pi/\beta} \times t_{\max}^{3/2}Q_{\max}$ $\exp\left(\beta/t_{\max} + t_{\max}/\alpha - 2\sqrt{\beta/\alpha}\right)$. Given the saddle point method is an approximation, we numerically demonstrated its validity for a large range of α and β values.

References

Arfken, G. B., H. J. Weber, and F. E. Harris (2012), *Mathematical Methods for Physicists: A Comprehensive Guide*, Academic, San Diego, Calif.

Baeck, M. L., and J. A. Smith (1998), Rainfall estimation by the WSR-88D for heavy rainfall events, *Weather Forecast.*, 13(2), 416–436, doi:10.1175/1520-0434(1998)013<0416:rebtwf>2.0.co;2.

Beven, K., and A. Binley (1992), The future of distributed models—Model calibration and uncertainty prediction, *Hydrol. Process.*, 6(3), 279–298, doi:10.1002/hyp.3360060305.

Black, J., and T. A. Endreny (2006), Increasing stormwater outfall duration, magnitude, and volume through combined sewer separation, J. *Hydrol. Eng.*, 11(5), 472–481, doi:10.1061/(ASCE)1084-0699(2006)11:5(472).

Brocca, L., F. Melone, and T. Moramarco (2011), Distributed rainfall-runoff modelling for flood frequency estimation and flood forecasting, *Hydrol. Process.*, 25(18), 2801–2813, doi:10.1002/hyp.8042.

Brutsaert, W. (2005), *Hydrology: An Introduction*, Cambridge Univ. Press, New York.

Carpenter, T. M., J. A. Sperfslage, K. P. Georgakakos, T. Sweeney, and D. L. Fread (1999), National threshold runoff estimation utilizing GIS in support of operational flash flood warning systems, *J. Hydrol.*, 224(1/2), 21–44, doi:10.1016/s0022-1694(99)00115-8.

Chaplot, V., and C. Walter (2003), Subsurface topography to enhance the prediction of the spatial distribution of soil wetness, *Hydrol. Process.*, 17(13), 2567–2580, doi:10.1002/hyp.1273.

Criss, R. E., and W. E. Winston (2003), Hydrograph for small basins following intense storms, *Geophys. Res. Lett.*, 30(6), 1314, doi:10.1029/2002GL016808.

Criss, R. E., and W. E. Winston (2008a), Discharge predictions of a rainfall-driven theoretical hydrograph compared to common models and observed data, *Water Resour. Res.*, 44, W10407, doi:10.1029/2007WR006415.

Criss, R. E., and W. E. Winston (2008b), Properties of a diffusive hydrograph and the interpretation of its single parameter, *Math. Geosci.*, 40(3), 313–325, doi:10.1007/s11004-008-9145-9.

Deming, D., J. H. Sass, A. H. Lachenbruch, and R. F. De Rito (1992), Heat flow and subsurface temperature as evidence for basin-scale groundwater flow, North Slope of Alaska, Geol. *Soc. Am. Bull.*, 104(5), 528–542, doi:10.1130/0016-7606(1992)104<0528:HFASTA>2.3.CO;2.

Doherty, J. (2001), *PEST Surface Water Utilities User's Manual*, Watermark Numer. Comput., Brisbane, Qld, Australia.

Easton, Z. M., P. Gerard-Marchant, M. T. Walter, A. M. Petrovic, and T. S. Steenhuis (2007), Hydrologic assessment of an urban variable source watershed in the northeast United States, *Water Resour. Res.*, 43, W03413, doi:10.1029/2006WR005076.

Endreny, T., and V. Collins (2009), Implications of bioretention basin spatial arrangements on stormwater recharge and groundwater mounding, *Ecol. Eng.*, 35(5), 670–677, doi:10.1016/j.ecoleng.2008.10.017.

García, J., J. Chiva, P. Aguirre, E. Álvarez, J. P. Sierra, and R. Mujeriego (2004), Hydraulic behaviour of horizontal subsurface flow constructed wetlands with different aspect ratio and granular medium size, *Ecol. Eng.*, 23(3), 177–187, doi:10.1016/j.ecoleng.2004.09.002.

Georgakakos, K. P. (1986), A generalized stochastic hydrometeorological model for flood and flash-flood forecasting: 1. Formulation, *Water Resour. Res.*, 22(13), 2083–2095, doi:10.1029/WR022i013p02083.

Hapuarachchi, H. A. P., Q. J. Wang, and T. C. Pagano (2011), A review of advances in flash flood forecasting, *Hydrol. Process.*, 25(18), 2771–2784, doi:10.1002/hyp.8040.

Hrachowitz, M., C. Soulsby, D. Tetzlaff, I. Malcolm, and G. Schoups (2010), Gamma distribution models for transit time estimation in catchments: Physical interpretation of parameters and implications for time-variant transit time assessment, *Water Resour. Res.*, 46, W10536, doi:10.1029/2010WR009148.

Hsu, K. L., H. V. Gupta, and S. Sorooshian (1995), Artificial neural-network modeling of the rainfall-runoff process, *Water Resour. Res.*, 31(10), 2517–2530, doi:10.1029/95WR01955.

Javier, J. R. N., J. A. Smith, K. L. Meierdiercks, M. L. Baeck, and A. J. Miller (2007), Flash flood forecasting for small urban watersheds in the Baltimore metropolitan region, *Weather Forecast.*, 22(6), 1331–1344, doi:10.1175/2007waf2006036.1.

Kirchner, J. W., X. Feng, and C. Neal (2001), Catchment-scale advection and dispersion as a mechanism for fractal scaling in stream tracer concentrations, *J. Hydrol.*, 254(1), 82–101, doi:10.1016/S0022-1694(01)00487-5.

Krzysztofowicz, R. (1999), Bayesian theory of probabilistic forecasting via deterministic hydrologic model, *Water Resour. Res.*, 35(9), 2739–2750, doi:10.1029/1999WR900099.

Lee, H., E. Zehe, and M. Sivapalan (2007), Predictions of rainfall-runoff response and soil moisture dynamics in a microscale catchment using the CREW model, *Hydrol. Earth Syst. Sci.*, 11(2), 819–849, doi:10.5194/hess-11-819-2007.

Liu, Y., S. Gebremeskel, F. De Smedt, L. Hoffmann, and L. Pfister (2003), A diffusive transport approach for flow routing in GIS-based flood modeling, *J. Hydrol.*, *283*(1–4), 91–106, doi:10.1016/S0022-1694(03)00242-7.

Marsalek, J., and B. Chocat (2002), International report: Stormwater management, *Water Sci. Technol.*, *46*(6/7), 1–17.

Martina, M. L. V., E. Todini, and A. Libralon (2005), A Bayesian decision approach to rainfall thresholds based flood warning, *Hydrol. Earth Syst. Sci.*, *10*(3), 413–426, doi:10.5194/hessd-2-2663-2005.

McDonnell, J. J. (1990), A rationale for old water discharge through macropores in a steep, humid catchment, *Water Resour. Res.*, *26*(11), 2821–2832, doi:10.1029/WR026i011p02821.

Nash, J. E., and J. V. Sutcliffe (1970), River flow forecasting through conceptual models. I. A discussion of principles, *J. Hydrol.*, *27*(3), 282–290, doi:10.1016/0022-1694(70)90255-6.

Ntelekos, A. A., K. P. Georgakakos, and W. F. Krajewski (2006), On the uncertainties of flash flood guidance: Toward probabilistic forecasting of flash floods, *J. Hydrometeorol.*, *7*(5), 896–915, doi:10.1175/jhm529.1.

Ogden, F. L., H. O. Sharif, S. U. S. Senarath, J. A. Smith, M. L. Baeck, and J. R. Richardson (2000), Hydrologic analysis of the Fort Collins, Colorado, flash flood of 1997, *J. Hydrol.*, *228*(1/2), 82–100, doi:10.1016/s0022-1694(00)00146-3.

Ogden, F. L., N. R. Pradhan, C. W. Downer, and J. A. Zahner (2011), Relative importance of impervious area, drainage density, width function, and subsurface storm drainage on flood runoff from an urbanized catchment, Water Resour. *Res.*, *47*, W12503, doi:10.1029/2011WR010550.

Perrin, C., C. Michel, and V. Andréassian (2001), Does a large number of parameters enhance model performance? Comparative assessment of common catchment model structures on 429 catchments, *J. Hydrol.*, *242*(3), 275–301, doi:10.1016/S0022-1694(00)00393-0.

Press, W. H., B. P. Flannery, S. A. Teukolsky, and W. T. Vetterling (1986), *Numerical Recipes*, Cambridge Univ. Press, New York.

Refsgaard, J. C. (1997), Parameterisation, *calibration and validation of distributed hydrological models*, J. Hydrol., *198*(1–4), 69–97, doi:10.1016/S0022-1694(96)03329-X.

Rinaldo, A., K. J. Beven, E. Bertuzzo, L. Nicotina, J. Davies, A. Fiori, D. Russo, and G. Botter (2011), Catchment travel time distributions and water flow in soils, *Water Resour. Res.*, *47*, W07537, doi:10.1029/2011WR010478.

Saint-Venant, B. (1871), Theory of unsteady water flow, with application to river floods and to propagation of tides in river channels, *Fr. Acad. Sci.*, *73*, 148–154.

Sansalone, J., X. Kuang, and V. Ranieri (2008), Permeable pavement as a hydraulic and filtration interface for urban drainage, *J. Irrig. Drain. Eng.*, *134*(5), 666–674, doi:10.1061/(ASCE)0733-9437(2008)134:5(666).

Schilling, J., and J. Logan (2008), Greening the Rust Belt: A green infrastructure model for right sizing America's shrinking cities, *J. Am. Plann. Assoc.*, *74*(4), 451–466, doi:10.1080/01944360802354956.

Smith, K., and R. Ward (1998), *Floods: Physical Processes and Human Impacts*, Wiley, Chichester, U. K.

Vogel, R. M., and C. N. Kroll (1992), Regional geohydrologic-geomorphic relationships for the estimation of low-flow statistics, *Water Resour. Res.*, *28*(9), 2451–2458, doi:10.1029/92WR01007.

Winchell, M., H. V. Gupta, and S. Sorooshian (1998), On the simulation of infiltration- and saturation-excess runoff using radar-based rainfall estimates: Effects of algorithm uncertainty and pixel aggregation, *Water Resour. Res.*, *34*(10), 2655–2670, doi:10.1029/98WR02009.

Yang, Y., T. A. Endreny, and D. J. Nowak (2011), i-Tree Hydro: Snow hydrology update for the urban forest hydrology model, *J. Am. Water Resour. Assoc.*, *47*(6), 1211–1218, doi:10.1111/j.1752-1688.2011.00564.x.

Yen, B., and C. W. S. Tsai (2001), On noninertia wave versus diffusion wave in flood routing, *J. Hydrol.*, *244*(1), 97–104, doi:10.1016/S0022-1694(00)00422-4.

Young, P. C. (2002), Advances in real-time flood forecasting, *Philos. Trans. R. Soc. Lond. Ser. A*, *360*(1796), 1433–1450, doi:10.1098/rsta.2002.1008.

Younis, J., S. Anquetin, and J. Thielen (2008), The benefit of high-resolution operational weather forecasts for flash flood warning, *Hydrol. Earth Syst. Sci.*, *12*(4), 1039–1051, doi:10.5194/hess-12-1039-2008.